Highly Linear Bipolar Transconductor For Broadband High-Frequency Applications with Improved Input Voltage Swing

Hsuan-Yu Marcus Pan and Lawrence E. Larson
University of California, San Diego
9500 Gilman Drive
La Jolla, CA, 92093, USA
hspan@ucsd.edu

***Abstract*—An all n-p-n highly linear wide-bandwidth bipolar transconductor (G_m) stage is presented based on a variation of Caprio's Quad. The high-frequency (HF) linearity of the improved G_m cell is examined by a Volterra analysis. The improved G_m cell has a higher input voltage swing range than other approaches.**

I. INTRODUCTION

Highly linear all n-p-n bipolar transconductors are widely used in many applications to provide faithful voltage-to-current conversion of input stages, such as continuous-time filters [1], mixers [2] and variable gain amplifiers [3]. To meet the required linearity specifications of G_m cells, various linearity enhancement techniques were developed, such as resistor degeneration [4-5], Caprio's Quad [6], feedback with operational amplifiers [7] and the Cascomp [8].

Because of the cross-coupled translinear configuration, Caprio's Quad has inherent base-emitter voltage (V_{BE}) cancellation and provides a very linear voltage-to-current conversion [9]. However, the input voltage swing is also limited due to its cross-coupled base-collector junctions. In light of this, a new bipolar transconductor is proposed based on Caprio's Quad to double the input voltage swing while the high linearity characteristic is maintained. The HF linearity of the improved G_m cell is investigated by a Volterra series analysis [11] and compared with the resistor degeneration technique and Caprio's Quad.

The paper is organized as follows: Section II describes the improved G_m cell's operation. Section III investigates its linearity properties. Section IV summarizes the noise performance. Section V calculates the figure-of-merit of each linearity enhancement technique, Conclusions are provided in Section VI.

II. PRINCIPLE OF OPERATION

The most popular linearization scheme of bipolar differential pairs is with an emitter degeneration resistor [4-5], which is shown in Fig. 1(a). The output current is the well-known

$$\Delta I = \frac{V_{in} + \Delta V_{BE}}{2R_{ee}} \tag{1}$$

where ΔV_{BE} represents the base-emitter voltage difference of Q_1 and Q_2. Equation (1) shows that the imperfect linearity results from the incomplete cancellation of base-emitter voltages of Q_1 and Q_2, i.e. V_{BE1} is not exactly equal to V_{BE2}.

To obtain improved cancellation of base-emitter voltages, Caprio's Quad added one cross-coupled pair Q_3-Q4 to the original differential pair Q_1-Q_2, as shown in Fig. 1(b) [6]. The loop voltage can be written as

$$V_{in} - V_{BE1} - V_{BE4} + 2R_{ee}\Delta I + V_{BE3} + V_{BE2} = 0 \tag{2}$$

Because of the cancellation of the base-emitter voltages of Q_1-Q_4, Caprio's Quad is very linear. Nevertheless, the input voltage swing range of Caprio's Quad is limited due to the cross-coupled base-collector junctions of Q_3 and Q_4. When V_{in} exceeds one junction turn-on voltage – roughly 0.8V – the base-collector junction of Q_3 will become forward-biased and high linearity operation will not be preserved.

To improve the input voltage swing range, a new G_m cell is proposed based on a variation of Caprio's Quad and shown in Fig. 1(c). The improved G_m cell is composed of two translinear loops: Q_1-Q_3-Q_4-Q_2 and Q_7-Q_5-Q_6-Q_8. The input voltage loop can be expressed as:

$$V_{in} - V_{BE1} - V_{BE3} - 2R_{ee}\Delta I + V_{BE4} + V_{BE2} = 0 \tag{3}$$

With the aid of the other translinear loop Q_7-Q_5-Q_6-Q_8, we have

$$V_{BE7} + V_{BE5} - V_{BE6} - V_{BE8} = 0 \tag{4}$$

Because of the cancellation of base-emitter voltages, the improved G_m cell preserves the highly linearity characteristics of Caprio's Quad. Moreover, the input voltage swing range is roughly doubled due to the aid of the second translinear loop. The base-collector junctions of Q_7-Q_3 and Q_4-Q_8 will not become forward-biased until V_{in} exceeds two V_{BE}'s – roughly 1.6V. Hence the input voltage swing range is doubled compared with Caprio's Quad.

1-4244-0921-7/07 $25.00 © 2007 IEEE.

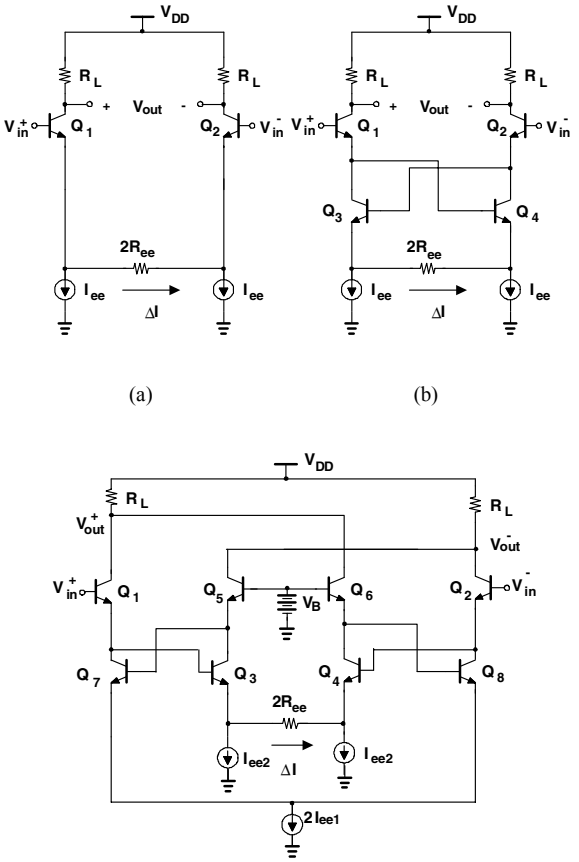

Fig.1 Different linearity enhancement techniques: (a) differential pair with emitter degeneration resistor (b) Caprio's Quad and (c) improved G_m cell.

III. LINEARITY

In communication applications, the linearity is usually characterized by intermodulation distortion (*IM*) and third-order input referred intercept point (*IIP3*) [10]. These weakly nonlinear HF characteristics can be calculated by the Volterra series method [11]. To simplify the Volterra analysis, the following assumptions are made: 1) Current gain is assumed very large, 2) Base-emitter capacitor C_{be} is estimated as g_m , where g_m is the transconductance and is the forward transit time of bipolar transistors [12], 3) The product $g_m R_{ee}$ is much greater than unity, 4) The ratio $\Delta f/f$ is much less than unity, where f is the input signal frequency and Δf is the frequency spacing of the two-tone signal, 5) The source impedance R_s is purely resistive (as it would be for broadband applications).

A. Linearity of Differential Pair with Degeneration Resistor

Suppose a two-tone signal with frequency components $\Delta f+f$ and f is fed into differential pair with degeneration resistor, as shown in Fig. 1(a), the third-order input referred intercept point voltage (*VIIP3*) at frequency $f+2\Delta f$ is [5]

$$VIIP3_{Deg} \approx 4V_T\left(1+\frac{I_T R_{ee}}{2V_T}\right)^{\frac{3}{2}} \tag{5}$$

where V_T is the thermal voltage, R_{ee} is the emitter degeneration resistor and $I_T=2I_{ee}$ is the overall current consumption of the differential pair. Equation (5) shows the well-known result that the $VIIP3_{Deg}$ relies on the product $I_T R_{ee}$.

B. Linearity of Caprio's Quad

Through a Volterra series analysis, the third-order intermodulation components (*IM3*) of the output voltage V_{out} at frequency $f+2\Delta f$ can be expressed as:

$$IM3_{Cap} \approx \left|\frac{A_{in}^2}{8g_m^3 R_{ee}^3 V_T^2}\frac{f}{f_T}\right| \tag{6}$$

where A_{in} is the input amplitude (in Volt), g_m is the transconductance of the transistors, and R_{ee} is the emitter degeneration resistor in Fig. 1(b). The quantify f_T is the cut-off frequency of the bipolar transistor, and is evaluated as $g_m/2\pi C_{be}$. *IIP3* can be solved from (6) by setting $IM3_{cap}$ =1 as follows:

$$VIIP3_{Cap} \approx 2\sqrt{2}V_T\sqrt{\frac{g_m{}^3 R_{ee}{}^3 f_T}{f}} \tag{7}$$

where $VIIP3_{cap}$ represents the third-order input referred intercept point voltage of Caprio's Quad. $VIIP3_{cap}$ can be further simplified as

$$VIIP3_{Cap} \approx \sqrt{\frac{f_T I_T{}^3 R_{ee}{}^3}{f V_T}} \tag{8}$$

where I_T is the overall current consumption. Compared with the differential pair with degeneration resistance, $VIIP3_{cap}$ is not only a function of the product $I_T R_{ee}$, but also a function of the frequency ratio f/f_T. It can be seen that the linearity can be further improved by using high f_T bipolar transistors.

C. Linearity of the Improved G_m Cell

The *VIIP3* of the improved G_m cell can be computed in a similar manner. Through a Volterra series analysis, the third-order intermodulation components (*IM3*) of output voltage V_{out} can be expressed as

$$IM3_{Imp} \approx \left|\frac{A_{in}^2}{32g_m^3 R_{ee}^3 V_T^2}\frac{f(K+1)^2}{f_T K^5}\right| \tag{9}$$

where g_m is the transconductance of Q1, Q2, Q7 and Q8. $K=I_{ee1}/I_{ee2}$ is the tail current source ratio in Fig. 1(c). The *IIP3* can be solved from (9) by setting $IM3_{Imp}$ =1 as follows:

$$VIIP3_{Imp} \approx 2\sqrt{2}V_T\sqrt{\frac{g_m{}^3R_{ee}{}^3K^5f_T}{(K+1)^2f}} \tag{10}$$

where $VIIP3_{Imp}$ represents the third-order input referred intercept point voltage of the improved G_m cell. $VIIP3_{Imp}$ can be further simplified as

$$VIIP3_{Imp} \approx \sqrt{\frac{I_T{}^3R_{ee}{}^3K^5f_T}{V_T(K+1)^5f}} \tag{11}$$

where I_T is the overall current consumption of the improved G_m cell. Equation (11) shows that the improved G_m cell has roughly the same *VIIP3* as Caprio's Quad in (8) with a large value of K. With a high f_T device, $VIIP3_{Imp}$ can become very large, which is similar to Caprio's Quad.

To validate our Volterra series calculation, the simulated and calculated *VIIP3* for Caprio's Quad and the improved G_m cell with the same overall power consumption are shown in Fig. 2. Simulation results show close agreement with calculation results.

For an ideal transconductor, a flat transconductance response with respect to input voltage is desired. To verify the improved input voltage swing range, the simulated normalized transconductance of the differential pair with emitter degeneration, Caprio's Quad and the improved G_m cell is shown in Fig. 3. To highlight the transconductance flatness, a 0.1% G_m compression point is adopted to define the input voltage swing range. It can be seen that the input voltage swing range of the improved G_m cell is roughly doubled, and is superior to either Caprio's Quad or the classic emitter degeneration transconductance cell.

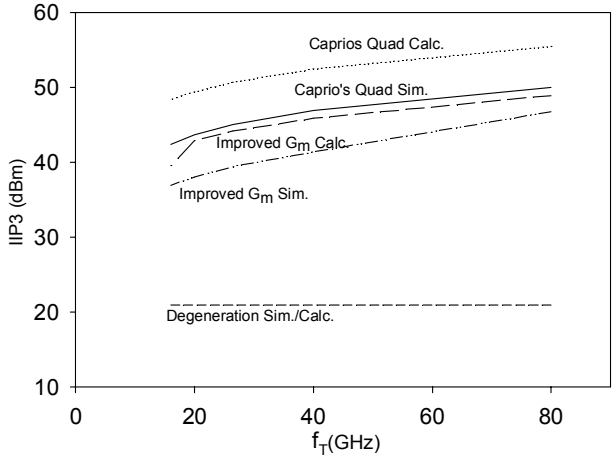

Fig. 2 IIP3 vs. cut-off frequency (f_T) of Caprio's Quad, improved G_m cell and differential pair with emitter degeneration at 20MHz. Simulation parameters : Ree=250 Ω, R_L=50Ω, K=2.8. Overall current consumption I_T=2mA.

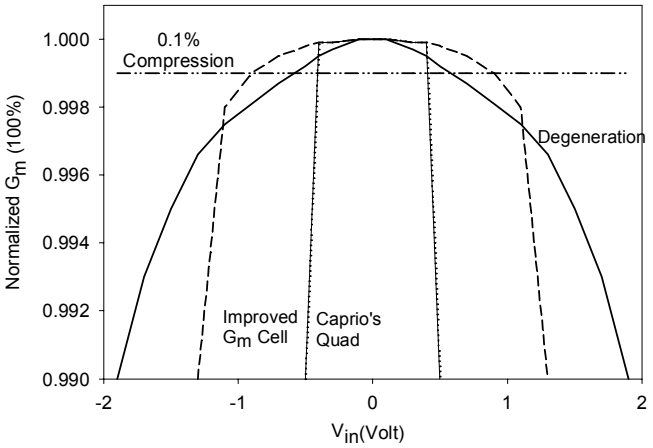

Fig. 3 Simulated normalized G_m vs. input voltage at 20MHz of Caprio's Quad, improved G_m cell and differnenail pair with emitter degeneration. The improved G_m cell has nearly a doubled input dynamic range compared with Caprio's Quad.

IV. Noise Performace

The minimum detectable signal of any circuit is usually limited by Noise Factor [13]. The Noise Factor of a differential pair with emitter degeneration resistor, Caprio's Quad and the improved G_m cell are

$$F_{Deg} = 1 + \frac{1}{2g_mR_s} + \frac{R_{ee}}{R_s} + \frac{1}{R_sR_L}\left(\frac{1+g_mR_{ee}}{g_m}\right)^2 \tag{12}$$

$$F_{Cap} = 1 + \frac{4g_mR_{ee}^2}{R_s(1+2g_mR_{ee})^2} + \frac{R_{ee}}{R_s} + \frac{2R_{ee}{}^2}{R_LR_s} \tag{13}$$

$$F_{Imp} = 1 + \left(\frac{K+1}{K}\right)\frac{1}{g_mR_s} + \frac{3R_{ee}}{R_s} + 2\left(\frac{K}{K+1}\right)^2\frac{R_{ee}{}^2}{R_sR_L} + \left(2K + \frac{K}{2(K+1)}\right)\frac{g_mR_{ee}{}^2}{R_s} \tag{14}$$

where F_{Deg} is the Noise Factor of the differential pair with emitter degeneration, F_{Cap} is the Noise Factor of Caprio's Quad, and F_{Imp} is the Noise Factor of the improved G_m cell. The base resistance r_b of bipolar transistors is ignored here to simplify the analysis. It can be seen that F_{Imp} is slightly higher than F_{Cap} and F_{Deg}, as expected.

V. Figure of Merit

A figure-of-merit (*FOM*) for a high-frequency amplifier was defined as follows [14]:

$$FOM_1 = 10\log\left(\frac{IIP3(mW)}{(F-1)}\frac{1}{P_{dc}(mW)}\right) \quad (15)$$

which normalizes the linearity, Noise Factor F and power consumption P_{dc}. However, the above *FOM* did not account for the input voltage swing range, which is an important characteristic. Hence, another *FOM* is proposed here to compare the transconductors' performance:

$$FOM_2 = 10\log\left(\frac{IIP3(mW)}{(F-1)}\frac{1}{P_{dc}(mW)}\frac{V_{swing}(Volt)}{V_{DD,\min}(Volt)}\right) \quad (16)$$

Where V_{swing}, defined by the 0.1% G_m compression point, represents the input swing range for circuit normal operation, and $V_{DD,min}$ is the minimum required supply voltage. The table of comparison at 20 MHz and 200MHz for emitter degeneration, Caprio's Quad and the improved G_m cell is shown in Table I. The improved G_m cell has a similar FOM to the Caprio's Quad but with doubled the input voltage swing range, which is a significant improvement for high-frequency applications.

TABLE I. TABLE OF COMPARISON FOR DIFFERENT TRANSCONDUCTORS

G_m Type	G_m Performance at 20MHz					
	IIP3 (dBm)	***NF (dB)***	***P_{dc} (mW)***	***V_{swing} (Volt)***	***$V_{DD,min}$ (Volt)***	***FOM (dB)***
Degeneration	20.9	4.9	6.0	0.6	0.9	8.1
Caprio's Quad	50.0	4.4	6.0	0.4	1.6	33.8
Improved G_m cell	46.7	6.5	6.0	0.9	1.6	31.0
G_m Type	**G_m Performance at 200MHz**					
	IIP3 (dBm)	***NF (dB)***	***P_{dc} (mW)***	***V_{swing} (Volt)***	***$V_{DD,min}$ (Volt)***	***FOM (dB)***
Degeneration	20.9	4.9	6.0	0.6	0.9	8.1
Caprio's Quad	39.8	4.4	6.0	0.4	1.6	23.6
Improved G_m cell	33.7	6.5	6.0	0.9	1.6	18.0

VI. CONLCUSION

An all n-p-n bipolar G_m cell is proposed based on a variation of Caprio's Quad. The HF linearity of the improved G_m cell is examined by Volterra analysis. Compared with Caprio's Quad, simulation results show the improved G_m cell has double the input voltage swing range and a similarly high linearity. The improved G_m cell is suitable for high-frequency broadband applications because of its high linearity and large input voltage swing range.

REFERENCES

[1] M. El-Gamal and G. W. Roberts, "Very high-frequency log-domain bandpass filter," IEEE Transactions on Circuits and Systems –II Analog and Digital Signal Processing, Vol. 45, No. 9, Sept. 1998, pp.1188-1198.

[2] L. Sheng and L. E. Larson, "An Si-SiGe BiCMOS direct-conversion mixer with second-order and third-order nonlinearity cancellation for WCDMA applications," IEEE Transactions on Microwave Theory and Techniques, Vol. 51, Issue.11, Nov. 2003, pp.2211 - 2220.

[3] A. Italia, E. Ragonese, L. L. Paglia and G. Palmisano, "A 5-GHz high-linear SiGe HBT up-converter with on-chip output balun," Proceedings of IEEE Radio Frequency Integrated Circuits Symposium, June 2004, pp.543 – 546.

[4] P. R. Gray, P. J. Hurst, S. H. Lewis, and R. G. Meyer, *Analysis and Design of Analog Integrated Circuits*, 4th edition, John Wiley & Sons Inc., 2001, pp. 215-252.

[5] A. A. Abidi, "General relations between IP2, IP3, and offsets in differential circuits and the effects of feedback," IEEE Transactions on Microwave Theory and Techniques, Vol. 51, Issue.5, May. 2003, pp. 1610-1612.

[6] R. Caprio, "Precision differential voltage-current convertor," IEE Electronics Letter, Vol. 9, no.6, Mar. 1973, pp. 147-149.

[7] S. Karvonen, T. Riley and J. Kostamovaara, "Highly linear G_m element for high-frequency applicatoins", Proceedings of IEEE International Midwest Symposium, Vol. 1, Dec 2003, pp. 145-148.

[8] P. A. Quinn, "A cascode amplifier nonlinearity correction technique", IEEE International Solid-State Circuits Conference Digest, Vol. 14, Feb. 1981, pp. 188-189.

[9] C. Toumazou, J. Lidgey and D. Haigh, *Analogue IC Design: the Current-Mode Approach*, Peter Peregrinus Ltd., 1990, pp. 71-74.

[10] B. Razavi, *RF Microelectronics*, Prentice Hall PTR, 1998, pp.17-22.

[11] P. Wambacq and W. M. C. Sansen, *Distortion Analysis of Analog Integrated Circuits*, Kluwer Academic Publishers, London, 1998.

[12] S. M. Sze, *Physics of Semiconductor Devices*, John Wiely & Sons Inc., 2nd Edition, 1981, pp. 133-189.

[13] T. H. Lee, *The Design of CMOS Radio-Frequency Integrated circuits*, Cambridge University Press, 1st edition, 1998, pp. 243-271.

[14] A. KarimiSanjaani, H. Sjoland and A. A. Abidi, "A 2GHz merged CMOS LNA and mixer for WCDMA," IEEE VLSI Circuits Technology Symposium Digest, June 2001, pp. 19-22.